MOORING LOADS OF A CIRCULAR NET CAGE WITH ELASTIC FLOATER IN WAVES AND CURRENT

Trygve Kristiansen[1,2] and Odd M. Faltinsen[1]
[1] Department of Marine Technology and Centre for Ships and Ocean Structures,
Norwegian University of Science and Technology (NTNU), Trondheim, Norway
[2] MARINTEK, Trondheim, Norway

ABSTRACT

This paper describes a study of an aquaculture net cage attached to a circular, flexible floater exposed to current and waves. Dedicated experiments are performed. Current is achieved by towing against the waves. The net cage is moored with four nearly horizontal moorings, and forces are measured in each mooring. Our recently implemented numerical model applies a screen type force model for the net, which earlier has been validated in current only. It is now applied also in combined current and waves. The code has been further developed such that it incorporates an elastic floater, modelled by a newly developed three-dimensional potential flow theory. The mean and total forces as well as the force amplitudes in the moorings are compared. Reasonable agreement is demonstrated for the mean and total forces.

KEYWORDS

Aquaculture fish farm; Net cage; Elastic floater; Screen model; Truss model; Waves and current

1 INTRODUCTION

Theoretical models and experiments for assessing both steady and unsteady hydrodynamic forces on fish farms have been presented during the past decades. It is a hydroelastic problem with a large number of moving components. A number of questions are still open as to *what factors are important* in modelling fish farms in waves and current. It is our overall intention to provide more knowledge in this direction. The total system with net cage, floater, mooring lines and bottom weights needs to be considered simultaneously. This requires a numerical model which has to be validated. Sensitivity studies may in turn be made using this model. This paper is intented to be a step towards a validated numerical model.

We consider a single, bottomless, circular net cage attached to a flexible floater exposed to both current and regular waves. Similar set-ups have been studied experimentally and numerically by[1] and[2], who both demostrate fair agreement between numerical calculations and experiments for the total mooring line forces.[3] also considered irregular waves.[4] studied numerically multiple net cages in waves. More references to relevant works are provided in these papers. Common to previous works is that a stiff floater is used, and further, there is a rather limitied number of wave/current conditions.

In the present paper we present a rather extensive and systematic set of wave/current conditions, and the floater is elastic. Dedicated experimental and numerical work are presented. In the numerical model we apply the three-dimensional linear potential theory presented by[5] for the floater, and the screen model for the viscous force on the net presented by[6].

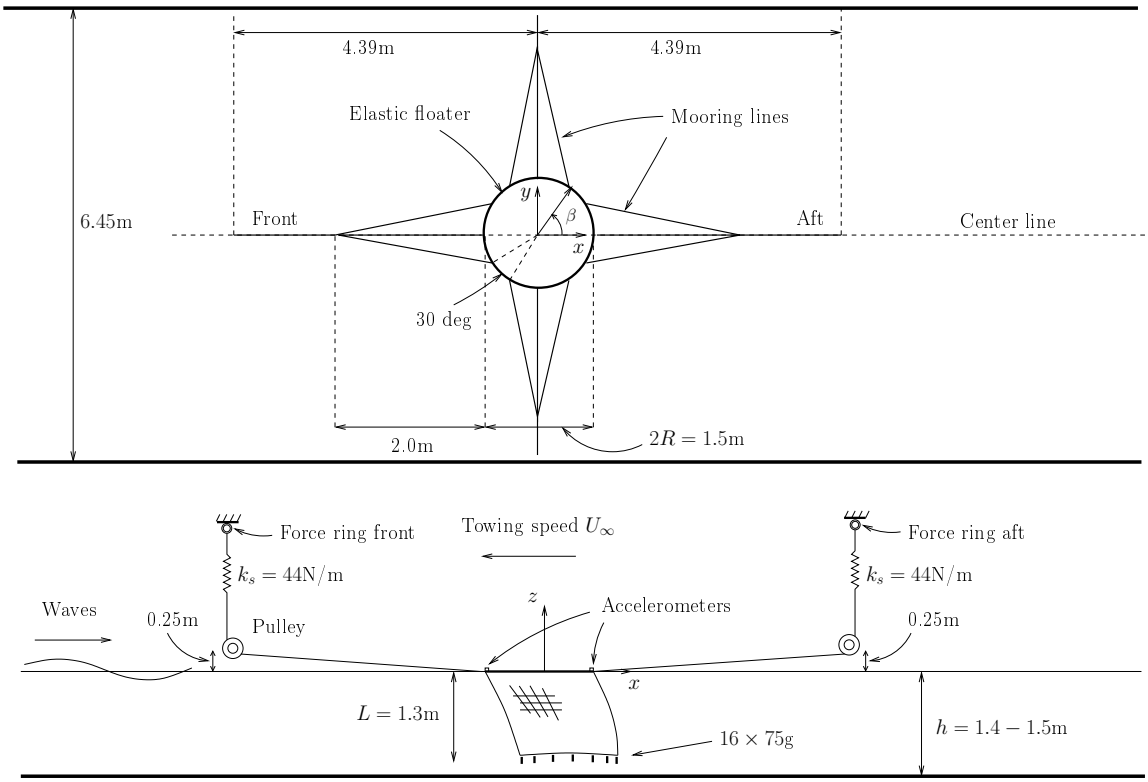

Figure 1: Experimental set-up. Upper: bird's eye view. Lower: side view. Tank length is 40m, width 6.45m and water depth 1.5m. A wave maker is located at the far left end of the tank and a parabolic beach at the far right end. The Cartesian coordinate system is located at the origin of the floater in calm conditions. The elastic floater is moored by four moorings; front, aft and two side moorings

2 EXPERIMENTS

We performed experiments in the Marine Cybernetics Lab at NTNU in Trondheim during the fall of 2011. The purpose of the experiments was primarily to obtain validation data, but also to study the system physically. Although we did not model a specific full scale system, the model and environment particulars were representative. Special attention was made to the structural bending stiffness. We chose a model test scale of 1:25. This model scale was suitable for the physical tank with respect to environmental parameters as well as model dimensions, and gave a realistic bending stiffness for the floater.

2.1 *Experimental set-up*

The experimental set-up is illustrated in Fig. 1 and additional measures are provided in Table 1. The mooring line forces were measured in each of the four moorings. The vertical motion at two points were measured by accelerometers; front and aft. Five wave gauges were used to measure the wave elevation. Two cameras were used to record the motion; one top view and one side view.

Care was made to avoid slack moorings, and in preserving a nearly circular shape of the floater during tests. In reality, the floater will ovalize in strong currents. However, the three-dimensional linear theory for the floater assumes perturbations around a circular floater. We constructed the following mooring set-up to achieve this. The floater was attached to the carriage by means of four nearly horizontal moorings with 12 fixed points with an equal spacing of 30 deg. In the front and aft moorings, there was a spring with spring constant $k_s = 44$N/m. This corresponds to a realistic full scale spring stiffness (27kN/m). The pre-tension was $T_p = 15N$. This corresponds to an unrealistically high full-scale value (230kN). The high pre-tension was necessary to avoid slack during testing and in order to keep the floater nearly circular. No springs were used in the side moorings, again in order to avoid strong ovalization.

TABLE 1:
MODEL PARTICULARS. MODEL SCALE 1:25. FROUDE SCALING IS USED

Description	Parameter	Model scale	Full scale
Floater diameter	D	1.5m	37.5m
Net depth	L	1.3m	32.5m
Cross-sectional diameter of floater	$2c$	30mm	0.75m
Floater bending stiffness	EI	0.136Nm^2	1.33×10^6 Nm^2
Net solidity ratios	Sn	0.26 and 0.32	0.26 and 0.32
Diameter of net twines	d_w	$\simeq 0.6 - 0.8$mm	-
Mass of bottom weights in air	M_{bw}	16×75g	16×1172kg
Spring stiffness (front and aft)	k_s	44N/m	27.5kN/m

The elastic floater model was made from a corrugated tube of the standard type used to cover electric cables in houses (see the photo in the left part of Fig. 2). This choice of material was a consequence of keeping a low cost. There were two outer cross-sectional diameters: 32mm and 26mm. An average diameter was estimated to be 30mm. The weight of the 16 sinkers were determined by requiring that the floater should be semi-submerged in calm conditions. In full scale the bottom weight per meter would be 159kg/m in air. The sinkers were made from lead.

Two nets were tested. The solidity ratios were Sn = 0.26 and Sn = 0.32. Both nets were bottomless, with a nominal diameter of 1.5m and depth of 1.3m. The 16 sinkers were attached directly to the bottom line of the net by clips. The nets were attached to the floater by 32 strips. When the model was in water, the net diameter at the top was measured to be 1.46m and the net depth was 1.27m.

2.2 *Test matrix*

The test matrix is presented in Table 2. The models were tested in three different main conditions: waves only, combined waves and current, and current only. The majority of the tests were made with the Sn = 0.26 net. The Sn = 0.32 net was tested in current only.

Waves were calibrated in the period range $T = 0.6 - 1.6$s with a step of 0.05s and with three wave height-to-wave length ratios: $H/\lambda = 1/60$, $1/30$ and $1/15$. The measured wave height was achieved within 97 - 99% of the desired value. Two-dimensionality of the waves was achieved (i.e. long-crested waves without transverse disturbances).

A selection of the tests were repeated at the end of the testing campaign. The repeatability was in general satisfactory, as may be seen from the results presented later.

Waves over-topping the floater occured in several tests. This ranged from only gentle over-topping to rather massive over-topping. This was found by visual inspection. A rough description is as follows. For

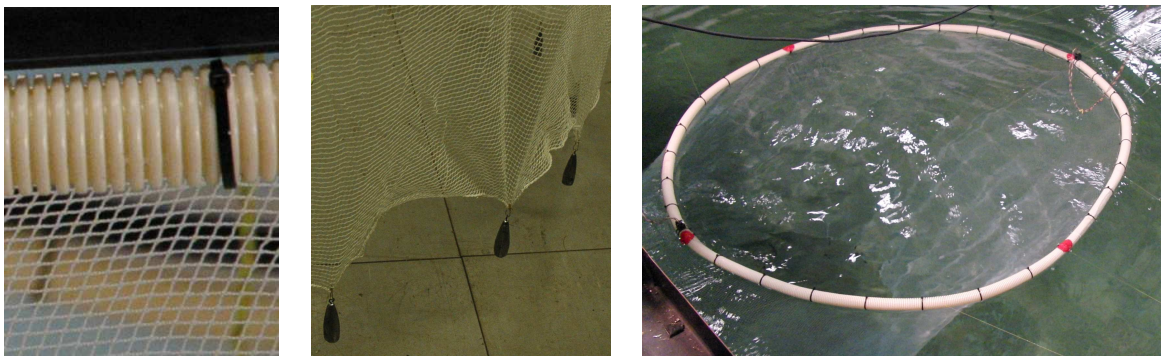

Figure 2: Left: photography of the floater (tube for electric cables) and the net with one of the 32 strips. Middle: Bottom weights (lead sinkers) and the net. Right: photography from a test with waves and current showing the elastic floater, the net, the mooring lines and the two accelerometers (front and aft)

TABLE 2:
TEST MATRIX. EXPERIMENTS CONDUCTED IN THE MC-LAB AT NTNU 2011

Solidity ratio Sn	**Current U_∞** [m/s]	**Wave steepness H/λ** 1/60	1/30	1/15
0.26	0	0.5 - 1.6s	0.5 - 1.6s	0.6 - 1.6s
	0.1	-	0.5 - 1.6s	0.6 - 1.6s
	0.2	-	0.5 - 1.6s	0.6 - 1.6s
	0.04 - 0.30	-	-	-
0.32	0.04 - 0.30	-	-	-

the $1/60$ steepness waves, no over-topping occured. For the $1/30$ steepness waves, over-topping occured for $\lambda/D \gtrsim 1$. For the $1/15$ steepness waves, over-topping occured for all wave periods, with massive over-topping for $\lambda/D \gtrsim 1.5$.

3 NUMERICAL METHOD

3.1 *The net*

To represent the net we use the truss model by[7], which was also applied by[6]. Illustrative snapshots are shown in Fig. 3. The net is represented by a mesh of $N_H \times N_V$ elastic trusses. The mooring lines are also represented by trusses. The springs in the front and aft mooring lines are modelled by elastic mooring trusses. The truss model is based on a kinematic constraint, which leads to a linear system of equations for the tensions in all net and mooring trusses. Once the tensions are solved for, these and the hydrodynamic forces on the net is used to time-step the nodes according to Newton's second law.

The viscous force on the net is represented by the screen type force model developed by[6]. We recapitulate the main particulars of the screen force model here. Each quadrilateral, defined by the truss system as illustrated in Fig. 3, is regarded as a flat screen. Each screen is characterized by its area A, the solidity ratio Sn, as well as an angle θ relative to the velocity. Further, the flow is characterized by the Reynold's number, Re, based on the physical twine diameter. In the screen model, the drag and lift coefficients are functions of Sn, Re and θ. The drag and lift forces are proportional to the square of the relative velocity, i.e.

$$F_D = \frac{1}{2}\rho A\, C_D(\mathrm{Sn}, \mathrm{Re}, \theta)|U_{\mathrm{rel}}|U_{\mathrm{rel}}, \quad F_L = \frac{1}{2}\rho A\, C_L(\mathrm{Sn}, \mathrm{Re}, \theta)|U_{\mathrm{rel}}|U_{\mathrm{rel}}, \tag{1}$$

where $U_{\mathrm{rel}} = (\mathbf{U}_\infty + \mathbf{u}_w - \mathbf{u}) \cdot \mathbf{n}$ is the relative velocity normal to the net panel. $\mathbf{U}_\infty$ is the ambient (current) velocity vector, $\mathbf{u}_w$ is the incident wave velocity vector and $\mathbf{u}$ the node velocity vector. Added mass loads on the net are secondary, and are simplified. The effect of the sum of the weight and buoyancy of the net is small and neglected.

We want to emphasize the following. (1) A common choice of force model for net cages in the literature is Morison type force models. These over-predict the forces when the net deforms appreciably. The present screen model yields more realistic forces. (2) Another force model that has been reported used is Darcy's law. One may not use the approximation applicable for porous media given by Darcy's law, where the force is linear in velocity, to represent the viscous forces on the net. The net does not represent a porous media, but rather a thin screen. In reality, the flow through a net experiences a pressure drop proportional to the velocity squared.

3.2 *The floater*

The kinematic constraint mentioned above involves the accelerations of each node (the nodes are the connections between the trusses). The accelerations of the nodes that represent the floater are found from the equations of motion for the floater, presented next. This means that there is a strong coupling between the motion of the floater and the net; both are solved for simultaneously.

The floater is assumed to be semi-submerged in still water conditions. It is further assumed to be perturbed around a circular shape, and is represented by sinusoidal modes in both the horizontal and the vertical directions. In addition to elastic motion, it is also allowed to undergo heave, pitch and surge. The

position of each point on the floater (x_f, y_f, z_f) is described by

$$x_f(\beta,t) = b_1(t) + v(\beta,t)\cos\beta, \quad y_f(\beta,t) = v(\beta,t)\sin\beta, \quad z_f(\beta,t) = \sum_{n=0}^{\infty} a_j(t)\cos n\beta, \tag{2}$$

where

$$v(\beta,t) = \sum_{n=2}^{\infty} b_j(t)\cos n\beta. \tag{3}$$

a_0 represents heave, a_1 pitch, a_2 the first vertical elastic mode etc., and b_1 represents surge, b_2 the first horizontal mode (ovalization) etc. The radial and vertical structural response is assumed to obey the following beam equations,

$$m\frac{\partial^2 v}{\partial t^2} + EI\left(\frac{\partial^4 v}{\partial s^4} + \frac{1}{R^2}\frac{\partial^2 v}{\partial s^2}\right) = f_r(s,t), \tag{4}$$

$$m\frac{\partial^2 z_f}{\partial t^2} + 2\rho c z_f + EI\frac{\partial^4 z_f}{\partial s^4} = f_z(s,t), \tag{5}$$

where m is the floater mass per unit length, EI the bending stiffness and $\partial/\partial s = R^{-1}\partial/\partial\beta$. β is explained in Fig. 1. f_r and f_z are the radial and vertical force per unit length of the floater, respectively, and include wave excitation force, added mass and hydrostatic restoring forces, and forces from the net cage and moorings. Damping forces (from wave radiation) are neglected.

For the wave excitation and added mass loads on the floater, linear potential flow theory is assumed. Deep water conditions and time-harmonic motions are considered. The added mass and wave excitation forces for the vertical modes ($n \geq 0$) are found using the recent zero-frequency, three-dimensional theory by[5]. Strip theory and long wave-length theory are assumed in the horizontal directions.

An error source in the hydrodynamic analysis of the floater is that frequency-dependent free-surface interactions occurs for wavelengths of the order of the floater diameter, D, according to potential flow theory. The consequence is that the added mass and damping coefficients vary strongly in our considered frequency range ([8]).

The equations of motion for radial mode b_n and vertical mode a_n are found as is usual within a modal approach, by multiplying by $\cos n\beta$ and integrating. The equation of motion for surge is posed separately due to the fact that the beam equation does not properly account for the inertia force. The infinite sums are truncated to a finite number of modes, denoted N_{mod}. The equations of motion then provide expressions for the accelerations at each floater node in the kinematic constraint for the total net-mooring-floater system.

4 RESULTS AND DISCUSSION

In this section, we present and compare results from the dedicated model tests and the present numerical simulations. We are able to predict the mean and total forces in the mooring lines in combined waves and current reasonably well. We first present comparisons in current only.

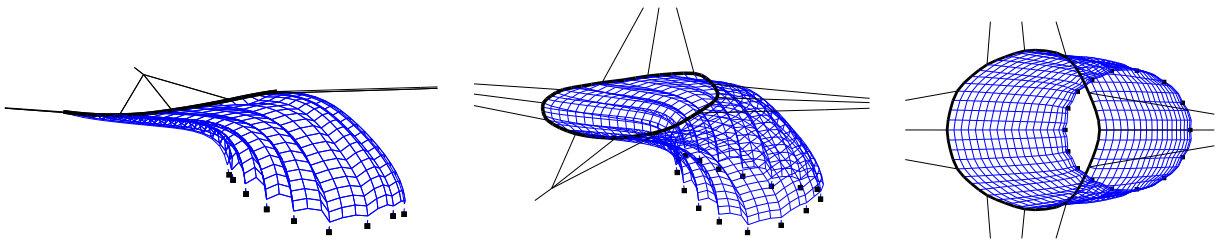

Figure 3: Snapshots from three different angles. Simulation with waves and current using the present numerical code: elastic floater, net, bottom weights and mooring lines. $U_\infty = 0.2$m/s, $T = 1.35$s and $H/\lambda = 1/15$. $N_H \times N_V = 48 \times 18$

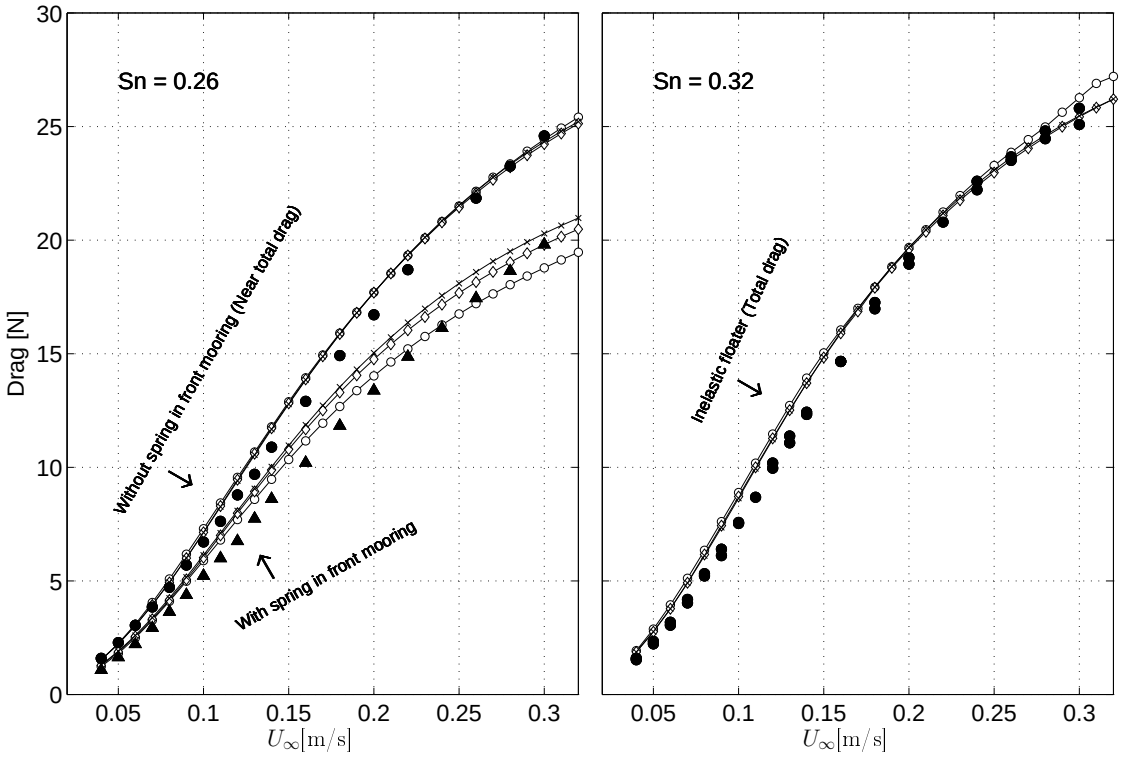

Figure 4: The mean force (drag) decuced from the front and aft mooring lines in current only. Filled symbols: experimental results. Triangular and circular symbols for Sn = 0.26 denote experiments with and without a spring in the front mooring line, respectively (elastic floater and four mooring lines in both cases). The filled symbols for Sn = 0.32 denote experiments with an inelastic floater moored only front and aft. Open symbols: present simulations, where circles represent 32×12 mesh, diamonds 48×18 mesh and x-symbols 64×24 mesh

4.1 *Current only*

The mean forces (the sum of the front and aft mooring line forces) are presented in Fig. 4. The filled symbols represent model tests, while the open symbols represent the numerical results, with three resolutions.

The Sn = 0.32 net was tested with a *stiff* floater moored only in the front and aft. Thus, all drag on the net is absorbed in the front and aft moorings, and the presented results represent the total drag. The tests were repeated, and we see that the repeatability was good. The Sn = 0.26 net was tested with the *elastic* floater only. The triangular symbols in the left sub-figure represent tests where the floater was moored as shown in Fig. 1, i.e. with springs in the front and aft moorings. Thus some horizontal drag force is absorbed in the side moorings from the offset caused by the drag. The offset length is denoted by x_{off}. The circular symbols represent tests were the front spring was removed. Thus, $x_{\text{off}} = 0$, and so, the majority of the drag force is believed to be absorbed by the front and aft mooring lines.

From Fig. 4 it is clear that the *total drag* is not sensitive to the grid, and that the 32×12 grid is sufficient, with a slight exception at the highest velocities on the Sn = 0.32 net. This is consistent with the convergence study in[6]. In the case that there is a spring in the front mooring line, the results do depend slightly on the resolution. A plausible explanation to this behaviour is that some force is absorbed in the side moorings, and we believe that the floater's ability to bend horizontally when the grid is too coarse is restricted.

The trend of the forces with respect to the current velocity is captured satisfactorily. However, the numerical results in general slightly over-predict. If we consider the $Sn = 0.26$ net with the 48×18 mesh we have the following: at $U = 0.1$m/s the mean mooring force is over-predicted by about 15% and 6% in the cases with and without spring in the front mooring, respectively. At $U = 0.2$m/s the numbers are 10% and 6%.

The differences between the two finest meshes are small. For the simulations with combined waves and current we chose the 48×18 mesh based on this. Due to the amount of simulations, the highest resolution

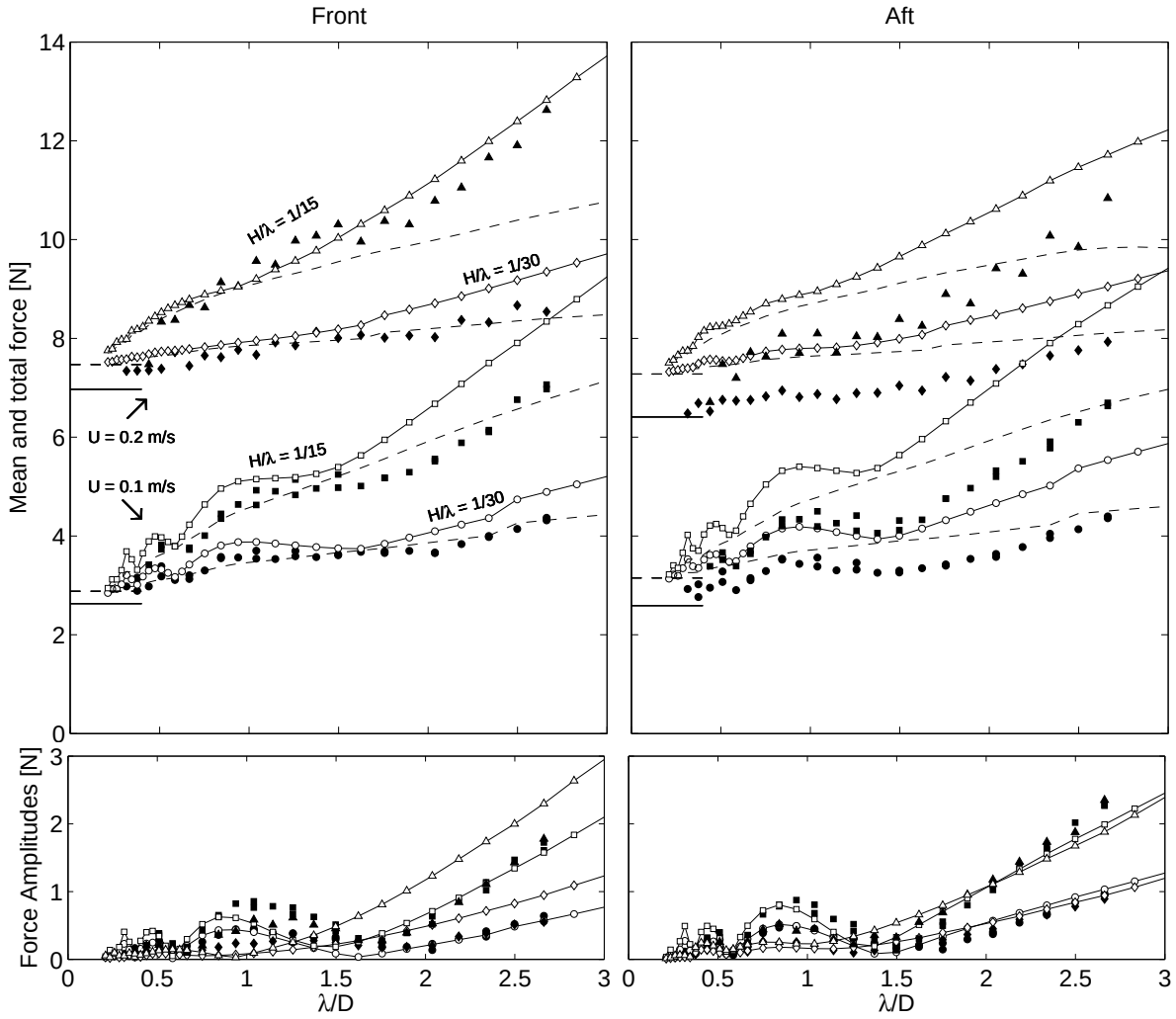

Figure 5: Forces in front (left) and aft (right) mooring lines. Sn = 0.26 net in combined current and waves. Filled symbols: experimental results. Open symbols: Present simulations with 48×18 mesh. Lower: Force amplitudes. Upper: Mean (dashed curves) and maximum (curves with open symbols) mooring line forces. Horizontal lines: mean mooring line tension in current only for experiments (solid lines) and simulations (dashed lines)

was not used. The simulations are quite time-consuming. The code is written in Fortran, but has not been optimized for high computational speed. With a 48×18 mesh, running 60 wave periods to reach steady-state takes 2 - 3 hours on a 2.4GHz laptop. The CPU time scales approximately with N^3, where N is the number of trusses.

4.2 *Current and waves*

In Fig. 5 we present mean force, total force and force amplitudes in the front and aft mooring lines in the four cases with combined waves and current listed in Table 2. The experimental data are represented by the filled symbols, while the numerical results are represented by the curves with open symbols. The mean forces (dashed curves) are shown only for the numerical results to avoid over-loading of the figures.

We note the following. (1) The different curves representing the force amplitudes are difficult to distinguish, but the main purpose of including these in the figure is to show that the force amplitudes are modest relative to the total forces. (2) The mean and total forces increase with increasing wave period. This is in particular noticable in the highest wave steepness cases ($H/\lambda = 1/15$). (3) The increase in the mean and total forces with increasing wave period is relatively speaking higher for the case with lowest current velocity.

For instance, the total force in the front mooring line is increased by a factor 2.3, from about 3N to 7N, when the longest wave of 1/15 steepness is added to the lowest current. The corresponding factor for the highest current is 1.8, (total force is increased from 7N to 12.5N).

Despite some over-prediction, the total force in the front mooring line is quite well predicted by the numerical simulations. In particular, the trend with respect to wave period is captured satisfactorily. The trend is captured also in the aft mooring line, although there is an appreciable over-prediction. The over-prediction increases somewhat with wave periods, but the majority is caused by the static current.

There are discrepancies in the force amplitudes, in particular in the front mooring line for the case with the highest current velocity ($U_\infty = 0.2$m/s). For the lowest current velocity case ($U_\infty = 0.1$m/s) the discrepancies are less pronounced, and in particular for the longest waves ($\lambda/D \gtrsim 1.5$).

4.3 *Sensitivity study*

We made a rather extensive sensitivity study using the 32×12 mesh (coarse mesh), and a more restricted study using the 48×18 mesh (fine mesh). The coarse mesh study was used for screening, while some selected parameters were varied in the fine mesh study. The observations from the fine mesh study was very similar to those from the coarse mesh study. The parameters that were varied are listed in Table 3, divided in five categories.

TABLE 3:
PARAMETERS THAT WERE VARIED IN THE SENSITIVITY STUDIES

Floater	**Net**	**Mooring**	**Environment**	**Numerical**
c	L	T_p	ω_e vs. ω_0	$N_H \times N_V$
R	E_{net}	k_s	x_{off}	N_{mod}
EI	Sn			
a_{33}^n	M_{net}			

We compared mean forces and force amplitudes. The main observations were that they were sensitive to only two parameters: the elasticity of the net, E_{net} and number of modes, N_{mod} (both vertical and horizontal) for the floater. We give a short discussion on these two and a selection of the other parameters.

In the nominal simulations, the net was treated as inelastic. The force amplitudes changed appreciably in the simulations with the elastic net, and also the mean forces were noticably affected. There is a question of what E_{net} should be. We applied $E_{\text{net}} = 5 \times 10^5 \text{Nm}^2$, which is two orders of magnitude smaller than that for nylon. Based on inspection of photos from our and similar experiments, where one sees arc-like shape of the bottom part of the net when sinker weighs are applied to it, it seems that the net inhibits a geometric elasticity. The applied value for E_{net} was chosen based on the similar arc-like static shape obtained in the numerical simulation. We are not confident that this is a correct modelling. A different structural elasticity modelling may be necessary. Therefore, we believe that the observed sensitivity to net elasticity is artificial, and further investigation necessary.

We applied the same number of modes vertically and horizontally. Simulations with $N_{\text{mod}} = 8$, 16 and 24 yielded practically identical behaviour. However, in simulations with $N_{\text{mod}} = 4$, the mooring forces were appreciably different, both force amplitudes and mean forces. It seems that $N_{\text{mod}} = 8$ is sufficient, at least in the present set-up.

Ultimately, it will be desirable to run simulations in irregular waves. However, it is uncertain how one may obtain retardation functions based on the highly oscillatory hydrodynamic coefficients for the vertical motion (see[8]). We were therefore in particular interested in how important the vertical motion is, and ran simulations reducing the vertical added mass, a_{33}^n, for all modes, to only 20% of their theoretical values. This had only a very small effect on the mooring forces. Using different values for the structural stiffness of the floater ($2EI$ and $0.5EI$) also gave very little effect.

We determined the offset, x_{off}, by first running the simulations to steady condition in current only, and then using the floater's mean position as origin when starting the waves. This was done in an attempt to obtain as correct as possible phasing between the wave induced forces on the floater and the wave induced, viscous forces on the net. Neither the mean mooring forces nor the force amplitudes were, however, sensitive to whether x_{off} was used or simply set to zero (still water position). The forces were neither sensitive to whether we applied the frequency of encounter, $\omega_e = \omega_0 + kU_\infty$ or the basic wave frequency ω_0.

We want to emphasize that we investigated the sensitivity on mooring loads, which is an integrated effect. For local effects, such as e.g. snap loads in support chains, some of the above parameters may be important.

5 CONCLUSIONS

We presented results from dedicated experiments at NTNU conducted 2011, and a newly developed numerical model of a circular aquaculture net cage with elastic floater in both current only as well as combined waves and current. We compared forces in the mooring lines, and demonstrated reasonable agreement for the mean and total forces, while there were noticable discrepancies in the force amplitudes. In the considered conditions, the mean forces dominate over the force amplitudes.

We presented a limited sensitivity study along with discussion on what factors are important in the modelling of circular, aquaculture fish farms. From 14 varied factors, only two were found to affect the forces in the mooring line significantly; the number of modes, N_{mod} (both vertical and horizontal) for the floater and the elasticity of the net, E_{net}. $N_{\text{mod}} = 8$ seemed to be adequate for our set-up. For $N_{\text{mod}} = 4$ the forces were appreciably different. The elasticity of the net was modelled in a crude manner (linear elastic with an artificially low E_{net}), and a different structural elasticity modelling is considered to be necessary in order to further investigate the effect of net elasticity.

The work is still ongoing. The discrepancies in the force amplitudes will be further investigated. A more extensive and detailed numerical sensitivity study will be presented in the future.

ACKNOWLEDGEMENTS

CREATE, Sintef Fisheries and Aquaculture provided financial support of the experiments.

REFERENCES

[1] Y-P. Zhao et al. "A numerical study on dynamic properties of the gravity cage in combined wave-current flow". In: *Ocean Engng.* 34 (2007), pp. 2350–2363.

[2] C-C. Huang, H-J. Tang, and J-Y. Liu. "Effects of waves and currents on gravity-type cages in the open sea". In: *Aquacultural Engng.* 38 (2008), pp. 105–116.

[3] G-H. Dong et al. "Numerical simulation of hydrodynamic behavior of gravity cage in irregular waves". In: *Aquacultural Engng.* 42 (2010), pp. 90–101.

[4] T-J. Xu et al. "Numerical investigation of the hydrodynamic behaviors of multiple net cages in waves". In: *Aquacultural Engng.* 48 (2012), pp. 6–18.

[5] O. M. Faltinsen. "Hydrodynamic aspects of a floating fish farm with circular collar". In: *26th Int. Workshop on Water Waves and Floating Bodies.* 2011.

[6] T. Kristiansen and O. M. Faltinsen. "Modelling of current loads on aquaculture net cages". In: *J. Fluids and Structures* Accepted for publication (2012).

[7] D. Marichal. "Cod-end numerical study". In: *3rd Int. Conf. on Hydroelasticity in Marine Technology, Oxford, UK.* 2003.

[8] P. Li and O. M. Faltinsen. "Wave-induced vertical response of an elastic circular collar of a floating fish farm". In: *Int. Conf. on Hydrodynamics (ICHD), St. Petersburg, Russia.* 2012.